Journal of Molecular Catalysis A: Chemical 326 (2010) 88–93

Contents lists available at ScienceDirect

Journal of Molecular Catalysis A: Chemical

journal homepage: www.elsevier.com/locate/molcata

^{1}H and ^{15}N chemical shifts of adsorbed acetonitrile as measures to probe the Brønsted acid strength of solid acids: A DFT study

Delian Yi [a], Hailu Zhang [b,*], Zongwu Deng [b]

[a] College of Chemical Engineering and Technology, Wuhan University of Science and Technology, Wuhan 430081, PR China
[b] Suzhou Institute of Nano-tech and Nano-bionics, Chinese Academy of Sciences, Suzhou 215125, PR China

ARTICLE INFO

Article history:
Received 24 December 2009
Received in revised form 21 April 2010
Accepted 22 April 2010
Available online 18 May 2010

Keywords:
Acid strength
DFT calculation
Solid acid
NMR chemical shift
Probe molecule

ABSTRACT

Isotropic chemical shift, a simple and uninterrupted NMR parameter, has been demonstrated to be a viable spectral scale to measure acid strength of solid acids. Here, the chemical shifts of acetonitrile interacting with modeled Brønsted acid sites were predicted by means of density functional theory (DFT) calculations. Results reveal linear correlations between ^{1}H (acidic proton) or ^{15}N chemical shift and proton affinity of Brønsted acid site, suggesting that the chemical shifts can be used to probe intrinsic Brønsted acid strength of solid acids. Steric effects of microporous solid acids on ^{1}H and ^{15}N chemical shifts were simulated by varying H···N distance or orientation of the C≡N bond in the $CH_3CN\cdots H^+$ adsorption complexes. Linear correlation is obtained between ^{1}H chemical shift and apparent acid strength regardless of the nature of the steric effect, while significant deviation occurs to ^{15}N chemical shift when the orientation of the C≡N bond is sharply deviated from its optimal orientation. The calculation results suggest that combination of ^{1}H and ^{15}N chemical shift can provide additional information on the structure of zeolite framework.

1. Introduction

Heterogeneous acidic catalysts such as zeolites, complex metal oxides, and heteropolyacid compounds have been widely used in environmentally benign synthesis of fine chemicals and petrochemicals [1–4]. The catalytic performance of these solid catalysts depends strongly on their acidity which has been extensively investigated using various analytic techniques, including Fourier transfer infrared spectroscopy, temperature-programmed desorption, photoelectron spectroscopy, microcalorimetry, etc. [4–7]. Recently, solid-state nuclear magnetic resonance (NMR) spectroscopy coupled with adsorption of probe molecules has also been demonstrated to be a viable technique for probing acidity of various solid catalysts [4,6–11]. For the solid-state NMR approach, the acid strength of different solid catalysts, especially the Brønsted acid strength, are often probed through measurement of relevant ^{1}H, ^{13}C, or ^{31}P NMR chemical shifts.

^{1}H NMR chemical shift of acidic proton is most often used to probe acid strength of solid catalysts, which is usually measured during adsorption of specific probe molecules, e.g. acetonitrile and pyridine (deuterated or undeuterated) [12–15]. It is well established that a downfield ^{1}H (acidic proton) chemical shift of $CH_3CN\cdots H^+$ complex induced by interaction between acetonitrile and acidic protons indicates stronger acid strength in microporous zeolites [12–14]. Chemical shifts of other nuclei, e.g. ^{13}C of adsorbed 2-^{13}C-acetone, or ^{31}P of trialkylphosphine oxides induced by interaction with acidic proton are also employed [9–11,16]. Nevertheless, each of these probe molecules has inherent advantages and disadvantages. For example, 2-^{13}C-acetone is used as probe molecule that yields a large ^{13}C resonance range (~30 ppm), but the S/N ratio of ^{13}C NMR spectroscopy is often reduced by the accompanied aldol reaction [9]. Adsorption of trialkylphosphine oxides on different solid acids can yield ^{31}P resonance of large chemical shift range (~40 ppm) without the need of isotope-labeling [16], but their large molecular size (>5.5 Å) limits their accessibility to acid sites in some micropores. Moreover, the solvent used in the adsorption process can be coadsorbed on the surface of solid acids, and may have undefined effect on the experimental results [17].

Recently, through density functional theory (DFT) theoretical calculation conducted on seven high-silica zeolites of different structures with and without adsorption of acetonitrile, Bell and coworkers demonstrated that isotropic chemical shifts of Brønsted proton (^{1}H) and nitrile nitrogen (^{15}N) of acetonitrile are well correlated with the hydroxyl bond length (r_{O-H}) of acetonitrile/Brønsted acid adsorption complexes, and hence with acid strength of the relevant zeolites [14]. A downfield shift of ^{1}H resonance and an upfield shift of ^{15}N resonance correspond to an increase in acid strength. Theoretically, adsorption of ^{15}N-labeled acetonitrile on some zeolites could yield chemical shift for ^{15}N resonance in a much larger range (~40 ppm) than ^{1}H resonance [14]. The calculation results suggest that acetonitrile is a good probe molecule to measure acid strength of solid catalysts through ^{1}H and ^{15}N NMR chemical shifts.

* Corresponding author. Tel.: +86 512 6287 2631; fax: +86 512 6287 2559.
E-mail address: hlzhang2008@sinano.ac.cn (H. Zhang).

1381-1169/$ – see front matter © 2010 Elsevier B.V. All rights reserved.
doi:10.1016/j.molcata.2010.04.012

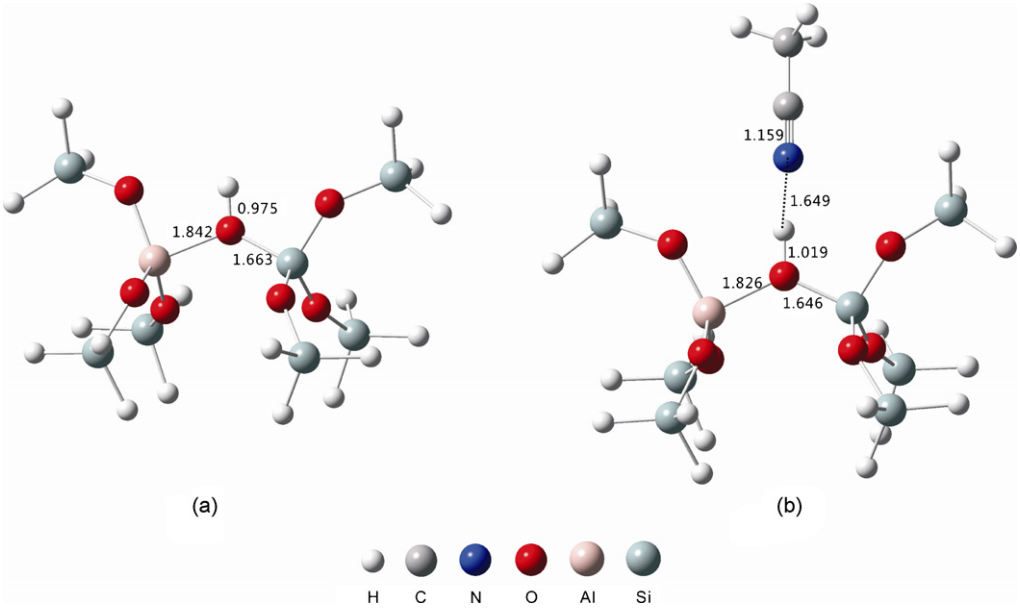

Fig. 1. (a) PW91/DNP-optimized modeled 8T zeolite structure and (b) equilibrium configuration of acetonitrile adsorbed on the solid acid model with a Si–H bond length (r_{Si-H}) of 1.50 Å. The relevant inter-atomic distances are in Å.

However, the zeolite structures used for the calculations are different in both intrinsic acid strength and topology. Hence, the calculations yielded virtually apparent acid strength of relevant zeolites, which is well correlated with the hydroxyl bond length and includes contribution from both intrinsic acid strength and steric effects. It is widely believed that geometric structure of adsorbed species on acid sites of microporous zeolite could be mediated by the topology of zeolite framework [18,19], which may be manifested in NMR chemical shift of relevant resonance. In this respect, it is necessary to distinguish the contribution of steric effects from that of intrinsic acid strength in order to gain a full understanding of the catalytic function of acid zeolites. On the other hand, zeolites represent a type of strong solid acids. It is also necessary to clarify whether such correlation also works for superacidic and weak solid acids when acetonitrile is used as a probe molecule since a downfield ^{1}H chemical shift is found to correspond to weaker acid strength when d_5-pyridine is selected as probe molecule [15], in contrast to experimental and theoretical results of acetonitrile.

In this contribution, we present an investigation on the correlations between intrinsic acid strength of solid acids and NMR chemical shifts of ^{1}H and ^{15}N resonances by using DFT calculation on modeled 8T zeolite clusters and acetonitrile as probe molecule. Modeled 8T zeolite clusters are selected to represent Brønsted acid of free micropore so that steric effect can be neglected. A Brønsted acid is defined as any chemical species (molecule or ion) that is able to lose, or donate a hydrogen ion (proton). Its intrinsic acid strength is well correlated to its proton affinity (PA) [20]. The latter is defined as the energy difference between protonated (S–OH) and deprotonated solid catalyst (S–O$^-$) (PA = E_{S-OH}–E_{S-O^-}): the smaller the PA value, the more easily the acidic proton is deprotonated, and thus the stronger the intrinsic acid strength. Recently, theoretical calculations have established a linear correlation between PA of modeled Brønsted acid sites and ^{1}H chemical shifts of adsorbed deuterated pyridine as well as ^{31}P chemical shifts of adsorbed trialkylphosphine oxides by using an 8T model cluster (free of steric effect) [15,16,21]. In this work, we try to correlate PA of model zeolites with both ^{1}H and ^{15}N NMR chemical shifts of adsorbed acetonitrile to probe Brønsted acid strength of solid acids from weak, strong to superacidic. In addition, we also try to simulate and evaluate the steric effect on ^{1}H and ^{15}N NMR chemical shifts by varying relevant bond length and orientation of acetonitrile adsorbed on the modeled 8T zeolite clusters.

2. Computational details

Modeled 8T zeolite clusters (Fig. 1a), $(H_3SiO)_3$–Si–OH–Al–$(OSiH_3)_3$, with different terminal Si–H bond lengths were used to represent solid acid sites with different intrinsic acid strengths. The Al12–O24–(H)–Si12 subgroups of ZSM-5 located at the intersections of the straight and zigzag channels were selected as the incipient structure of the modeled cluster. The validity of this method has been demonstrated by Kramer and Zheng's recent work [15,16,21,22]. All terminal hydrogen atoms in the clusters that take the places of corresponding O–Si bonds of a zeolite network are located at a Si–H distance of r_{Si-H} Å from the corresponding silicon atoms, and are oriented in their represented Si–O bond direction. The r_{Si-H} distances were set at 1.25, 1.50, 1.75, 2.00, 2.25, and 2.50 Å to represent six solid acids with increasing acid strength from weak, strong to superacidic. Partial optimization was performed to obtain configurations with minimum energy by allowing the O_3–Si–OH–Al–O_3 cluster to relax while keeping the angles (orientation) of the H_3 groups on the peripheral Si atoms fixed.

The geometrical parameters and Mulliken charge distribution of the modeled solid acid clusters with and without acetonitrile adsorption were optimized with the Dmol3 program [23–25], using a PW91 density function and the DNP basis set [26,27], during which the terminal H_3 groups on the peripheral Si atoms were also kept fixed. ^{1}H and ^{15}N isotropic chemical shifts were calculated at the B3LYP/6-311G(d, p) level by the Gauge-Independent Atomic Orbital (GIAO) method [28–30]. The ^{1}H and ^{15}N chemical shift parameters are referred to TMS and NH_3, respectively. The chemical shift calculations were performed using a Gaussian03 program package [31].

To simulate and evaluate the steric hindrance caused by the framework of microporous materials, further calculations were conducted on the 8T model with fixed $(H_3SiO)_3$–Si–O–Al–$(OSiH_3)_3$ zeolite geometry and varying H···N distances ($r_{H\cdots N}$) or orientations of the C≡N bond (∠(C≡N···H)) of acetonitrile. The 8T cluster

Table 1
O–H bond length (r_{O-H}), charge distribution on acidic proton, ^{1}H (acidic proton) chemical shift and proton affinities (PA) of the modeled acidic zeolites with different terminal Si–H bond lengths (r_{Si-H}).[a]

r_{Si-H}	r_{O-H}	H charge	$\delta(^1H)$	PA
1.25	0.974	0.371	4.1	326.8
1.50	0.975	0.371	4.2	296.2
1.75	0.975	0.380	4.3	282.2
2.00	0.976	0.384	4.4	269.2
2.25	0.977	0.384	4.5	258.0
2.50	0.978	0.384	4.7	249.7

[a] Bond length in Å, charge distribution in |e|, chemical shift in ppm, and proton affinity in kcal/mol.

Table 2
O–H bond length (r_{O-H}), N···H hydrogen bond length ($r_{N\cdots H}$), charge distribution on acidic proton and nitrile nitrogen, ^{1}H (acidic proton) and ^{15}N chemical shifts of $CH_3CN\cdots H^+$ adsorption complexes.[a]

r_{Si-H}	r_{N-H}	$r_{O\cdots H}$	H charge	N charge	$\delta(^1H)$	$\delta(^{15}N)$
1.25	1.699	1.010	0.467	−0.370	8.7	273.4
1.50	1.649	1.019	0.472	−0.383	9.7	268.0
1.75	1.579	1.031	0.476	−0.395	10.8	262.0
2.00	1.542	1.047	0.477	−0.404	12.0	255.4
2.25	1.492	1.063	0.476	−0.411	13.1	249.3
2.50	1.463	1.077	0.474	−0.415	14.0	244.7

[a] Bond length in Å, charge distribution in |e|, and chemical shift in ppm.

was fixed at r_{Si-H} = 1.50 Å (denoted as *f*8T model) as a reference configuration, and the configuration of $CH_3CN\cdots H^+$ adsorption complex was optimized with varying $r_{H\cdots N}$ and ∠(C≡N···H). The variation ranges of $r_{H\cdots N}$ and ∠(C≡N···H) were referred to Ref. [14].

3. Results and discussion

Fig. 1a shows the optimized equilibrium configuration of typical 8T cluster model with a Si–H bond length of 1.50 Å. The PA values, acidic bridging hydroxyl bond lengths, charge distributions on acidic protons as well as ^{1}H chemical shifts were calculated for all the six model bare zeolites and summarized in Table 1. The calculated PA values and O–H bond lengths of the bridging hydroxyl groups are in good agreement with previous report [21], and the calculated ^{1}H chemical shifts are also in a reasonable range as acidic zeolites usually raise ^{1}H resonances in the range of 3.7–5.2 ppm. Generally, an increase in O–H bond length or ^{1}H chemical shift indicates enhancement of Brønsted acid strength. Hence, the slight increases in calculated O–H bond length from 0.974 to 0.978 Å and ^{1}H chemical shift from 4.1 to 4.7 ppm with increase in Si–H bond length of the bare clusters from 1.25 to 2.50 Å as shown in Table 1 are in qualitative agreement with an increase in intrinsic acid strength of the model clusters from weak, strong to superacidic.

Upon adsorption of acetonitrile, the calculated O–H bond length further increases as a result of interaction between the acidic hydrogen and the nitrogen atom of acetonitrile as shown in Fig. 1b and Table 2. The magnitude of the O–H bond length increase depends on the acid strength of the model acidic sites, from ~3.7% to ~10.1% with increase in Si–H bond length from1.25 to 2.50 Å. The increase in O–H bond length is accompanied by a shortening of the formed N···H hydrogen bond length from 1.699 to 1.463 Å. This is understandable because acetonitrile is a weak basic molecule with a PA value of 186.4 kcal/mol [32]. Its partially negative-charged nitrogen atom can serve as proton acceptor to form hydrogen bond with the Brønsted acid site (refer Fig. 1b). Generally, a stronger Brønsted acid site results in a stronger hydrogen bonding between the nitrile nitrogen of acetonitrile and the acidic proton, and consequently a shorter hydrogen bond (N···H) length and a longer O–H bond length of the bridging hydroxyl group. The calculated minimum N···H bond length of 1.463 Å also suggests that the acidic proton is not completely transferred to acetonitrile so that no CH_3CNH^+ ion is formed.

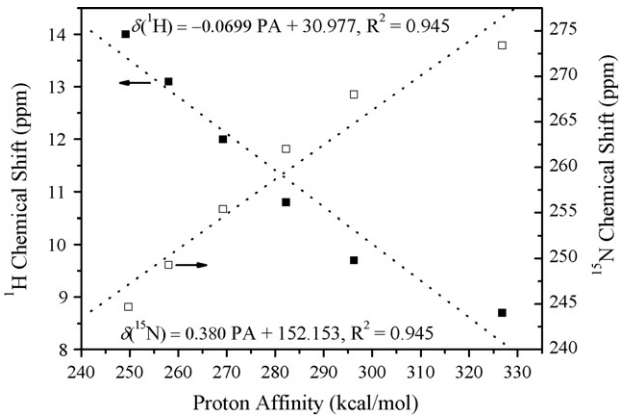

Fig. 2. Correlation of calculated ^{1}H (acidic proton, ■) and ^{15}N (□) chemical shifts of optimized $CH_3CN\cdots H^+$ complexes and proton affinities (PA) of modeled solid acid clusters.

When the hydrogen-bonded $CH_3CN\cdots H^+$ complex formed, the charge density around the nitrogen atom and the acidic proton should also exhibit change with change in acid strength. Our calculation indicates a monotonic increase in charge density around the nitrogen atom with increase in intrinsic acid strength (shown in Table 2 along with change in intrinsic acid strength as represented by different Si–H bond lengths). For the acidic proton, the charge density is influenced both by the adsorbed CH_3CN and the extent of deprotonation of different zeolite models, which leads to an irregular change in charge distribution around the H atom as also shown in Table 2.Change in charge density around a particular nucleus could be manifested in its NMR chemical shift. For example, increase in charge density around the nitrogen atom would lead to a more upfield ^{15}N chemical shift. Theoretically, DFT quantum chemical calculations offer an opportunity to predict chemical shifts based on the optimized electronic structures and the derivation of electronic wavefunctions. The ^{1}H (acidic proton) and ^{15}N chemical shifts of adsorbed $CH_3CN\cdots H^+$ complexes on modeled 8T zeolite clusters were calculated and also listed in Table 2. In order to explore the correlation between NMR chemical shifts of relevant nucleus and the proton affinities of solid acids, ^{1}H (acidic proton) and ^{15}N chemical shifts of the $CH_3CN\cdots H^+$ complexes were plotted versus proton affinities of modeled 8T zeolite clusters as shown in Fig. 2. Linear correlations are derived between the calculated PA and NMR chemical shifts.

$$\delta(^1H) = [-0.0699 \pm (0.0084)] \times PA + 30.977\,(\pm 2.733), \quad R^2 = 0.945 \tag{1}$$

$$\delta(^{15}N) = [0.380 \pm (0.046)] \times PA + 152.153\,(\pm 12.896), \quad R^2 = 0.945 \tag{2}$$

According to the calculation results, a larger ^{1}H chemical shift indicates a stronger intrinsic acid strength, in consistence with reported experimental results of apparent acid strength of microporous zeolites [12,13,33,34]. The ^{1}H chemical shifts fall into a range of 8–14 ppm, more downfield than resonance signals of both bare acidic protons (3.7–5.2 ppm) and methyl protons (~2 ppm) of acetonitrile. Hereby, deuteration of acetonitrile is not necessary when ^{1}H chemical shift is used to measure the acid strength despite possible overlapping among ^{1}H signals originating from methyl protons of acetonitrile, bare acidic protons, SiOH, and AlOH hydroxyl groups.

For ^{15}N-labeled acetonitrile, a smaller ^{15}N chemical shift corresponds to a stronger acid strength. The ^{15}N-labeled acetonitrile (^{15}N-acetonitrile) exhibits a much larger ^{15}N chemical shift range (~30 ppm) relative to ^{1}H chemical shift (~5.3 ppm) as acid strength

Table 3
O–H bond length (r_{O-H}), N···H hydrogen bond length ($r_{N\cdots H}$), ^{1}H (acidic proton) and ^{15}N chemical shifts of $CH_3CN\cdots H^+$ adsorption complexes at varying H···N distance or orientation of the C≡N bond.[a].

	r_{O-H}	$r_{H\cdots N}$	∠(C≡N···H)	$\delta(^1H)$	$\delta(^{15}N)$
Reference configuration[b]	1.019	1.649	173.2	9.7	268.0
$r_{H\cdots N}$ varied	1.077	1.400	177.6	13.7	255.2
	1.060	1.450	175.4	12.8	258.6
	1.046	1.500	175.1	12.0	261.5
	1.038	1.550	174.2	11.2	263.5
	1.028	1.600	173.7	10.4	265.9
	1.012	1.700	172.9	9.1	269.8
∠(C≡N···H) varied	1.019	1.649	180.0	9.7	268.4
	1.019	1.648	170.0	9.8	267.9
	1.019	1.649	160.0	9.8	267.3
	1.017	1.654	150.0	9.8	267.6
	1.017	1.659	140.0	9.8	268.5
	1.015	1.675	130.0	9.8	270.1
	1.007	1.759	120.0	8.9	274.4
	0.994	1.942	100.0	7.4	284.5

[a] Bond length in Å, bond angle in degree, chemical shift in ppm.
[b] Optimized configuration of $CH_3CN\cdots H^+$ adsorption complex with r_{Si-H} fixed at 1.50 Å.

of the model zeolite changes from weak, strong to superacidic. The linear correlation between PA of modeled 8T zeolite clusters and NMR chemical shifts of ^{1}H and ^{15}N resonances suggests that acetonitrile is a sensitive probe molecule for measuring intrinsic acid strength of solid acids.

In order to evaluate the contribution from steric effect of real zeolites to their measured apparent acid strength, DFT calculation was also conducted on an *f*8T zeolite cluster where r_{Si-H} was fixed at 1.50 Å (as a reference configuration) with H···N bond length varying from 1.400 to 1.700 Å or orientations of the C≡N bond as expressed by ∠(C≡N···H) varying from 100° to 180°. The fixed r_{Si-H} corresponds to a fixed PA value and thus fixed intrinsic acid strength. The steric effect was simulated by the varying H···N bond length or orientations of the C≡N bond. The calculation results were summarized in Table 3 along with that of the reference configuration. ^{1}H (acidic proton) and ^{15}N chemical shifts are further plotted versus r_{O-H}, $r_{N\cdots H}$ and ∠(C≡N···H) as shown in Figs. 3–5, respectively.

For the steric effect caused by varying H···N bond length, the calculation was conducted with H···N bond length fixed at specific values while optimizing r_{O-H} and other geometric parameters of adsorbed CH_3CN. Increase in H···N bond length from 1.400 to 1.700 Å is accompanied by corresponding shortening of 0.065 Å in O–H bond length, inferring gradual decrease in apparent acid strength. This is also manifested in a total decrease of

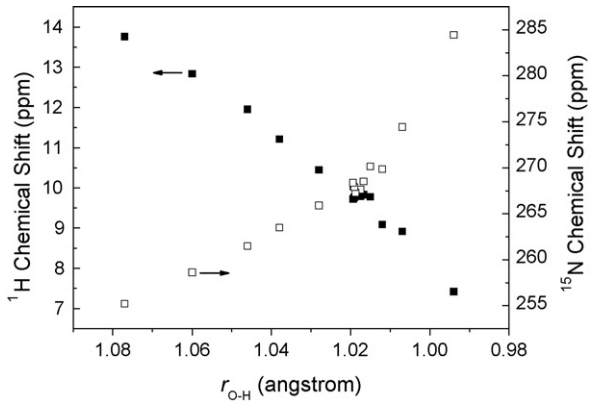

Fig. 3. Correlation of calculated ^{1}H (■), ^{15}N (□) chemical shifts and r_{O-H} of configuration restricted $CH_3CN\cdots H^+$ adsorption complexes.

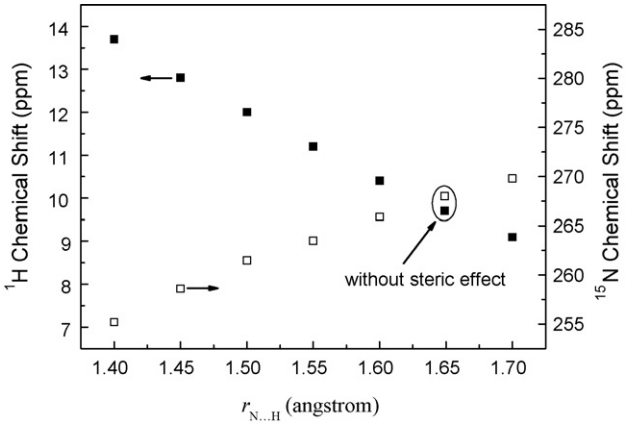

Fig. 4. Simulated steric effect on ^{1}H (■) and ^{15}N (□) chemical shifts of $CH_3CN\cdots H^+$ complexes caused by varying H···N distance.

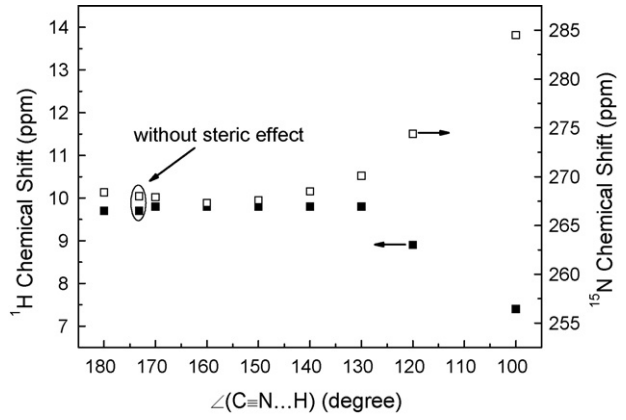

Fig. 5. Simulated steric effect on ^{1}H (■) and ^{15}N (□) chemical shifts of $CH_3CN\cdots H^+$ complexes caused by varying orientation of the C≡N bond.

4.6 ppm in ^{1}H chemical shift and a total increase of 14.6 ppm in ^{15}N chemical shift. Again, a linear correlation is obtained between relevant NMR chemical shifts and the apparent acid strength as shown in Fig. 3 (data with $r_{N\cdots H}$ between 1.012 and 1.077).

For the steric effect caused by varying orientations of the C≡N bond, the calculation was conducted with ∠(C≡N···H) fixed at specific values while optimizing r_{O-H} and the other geometric parameters of adsorbed CH_3CN. The calculation results demonstrate that when the orientation of the C≡N bond, i.e. ∠(C≡N···H), varies from 100° to 180°, a total increase of 2.4 ppm in ^{1}H chemical shift and a total decrease of 17.2 ppm in ^{15}N chemical shift is obtained, corresponding to an increase of 0.025 Å in hydroxyl bond length.

The above results indicate that upon adsorption of acetonitrile on zeolites, variation of H···N distances or orientation of the C≡N bond may give rise to significant change in geometric configuration of the adsorption complexes, including the O–H bond length (a measure of the apparent acid strength of solid acids), which is known as steric effect of zeolite's framework. Such steric effect is also manifested in electronic configuration of relevant nuclei and hence in their NMR chemical shifts, which exhibit correlation with the apparent acid strength of relevant zeolites, e.g. ^{1}H (acidic proton) and ^{15}N nucleuses in the present work. However, we also note that ^{1}H (acidic proton) chemical shift exhibits a linear correlation with the O–H bond length/apparent acid strength over the investigated range from 1.077 to 0.994 Å (Fig. 3) where the change from 1.077 to 1.012 is caused by variation of H···N distance and that

from 1.019 to 0.994 Å caused by variation of orientation of the C≡N bond (Table 3). This suggests that ^{1}H (acidic proton) chemical shift is correlated with apparent acid strength regardless of the nature of the steric effect.

^{15}N chemical shift is also correlated with the apparent acid strength, but in a more complex way depending on the nature of the steric effect. ^{15}N chemical shift is linearly correlated with apparent acid strength over the O–H bond length range of 1.077–1.012 (Fig. 3) caused by varying H···N distance, and exhibits similar steric effect as ^{1}H chemical shift (Fig. 4). When varying the orientation of the C≡N bond, however, it first exhibits a slight decrease when ∠(C≡N···H) varies from 180° to 160° followed by a gradual recovery when ∠(C≡N···H) further varies from 160° to 130°, whereas ^{1}H chemical shift exhibits no obvious change over the course (Fig. 5). When ∠(C≡N···H) further changes to 120° and 100°, significant chemical shift increase occurs to both ^{1}H and ^{15}N resonances, but with a much larger magnitude to ^{15}N than to ^{1}H (14.4 ppm/2.4 ppm in the course versus 14.6 ppm/4.6 ppm in the course of H···N distance variation). This is also manifested in the correlation between apparent acid strength and the calculated ^{1}H and ^{15}N NMR chemical shifts where ^{1}H chemical shift remains a similar linear correlation with apparent acid strength as that obtained in the course of H···N distance variation, whereas ^{15}N chemical shift exhibits a significant deviation from that obtained in the course of H···N distance variation (Fig. 3).

The significant deviation of ^{15}N chemical shift during variation of orientation of the C≡N bond may be explained qualitatively by the shielding and deshielding behavior of the ^{1}H and ^{15}N nuclei through transfer of electron density in the courses. Decrease in H···N distance should result in stronger interaction between hydroxyl hydrogen of zeolite and nitrile nitrogen of acetonitrile. This interaction, on one hand, results in electron density transfer from hydrogen to nitrogen as indicated by an increase in positive charge density at the H nucleus by ~1.5% (0.467 vs 0.474, Table 2) as the $r_{N–H}$ decreases from 1.699 to 1.463 Å with the absence of steric effect. Meanwhile, it may further induce significant electron density transfer from nitrile carbon to nitrile nitrogen through bonding electrons of the triple bond, particularly the π electrons, which may account for the much more significant increase in negative charge density at the N nucleus by ~12% (−0.370 vs −0.415, Table 2) (usually termed as a paramagnetic contribution to NMR chemical shift [35]). The overall results are a less shielded ^{1}H nucleus and a more shielded ^{15}N nucleus, and thus a downfield ^{1}H chemical shift and an upfield ^{15}N chemical shift. When the orientation of the C≡N bond deviates significantly from its optimal orientation (173.2°), the interaction is strongly disturbed by the steric constraint, and thus shift of electron density between hydroxyl hydrogen of zeolite and nitrile nitrogen of acetonitrile as well as the paramagnetic effect may be significantly weakened, which results in a significant deshielding of the ^{15}N nucleus and thus a downfield shift in much larger magnitude. In this case, ^{1}H nucleus exhibits a less significant increase in shielding due likely to the backshift of electron density from hydrogen to oxygen of the hydroxyl bond.

As a consequence, ^{1}H chemical shift exhibits a linear correlation with the apparent acid strength of zeolite regardless of the nature of steric effect, whereas ^{15}N chemical shift is linearly correlated with the apparent acid strength during variation of the H···N distance, but exhibits a significant deviation (in a much larger magnitude) when orientation of the probe molecule is deviated sharply from its optimal orientation. Hence, ^{15}N chemical shift is more sensitive to a steric effect caused by orientation of a probe molecule, which implies that a cross-analysis of ^{1}H and ^{15}N chemical shifts may provide additional information on the nature of the steric effect, and thus help understand the structure of zeolite framework.

4. Conclusion

Structures of modeled solid acids with different strength and acetonitrile adsorption complexes with and without steric effect, as well as the corresponding ^{1}H (acidic proton) and ^{15}N chemical shifts were calculated theoretically using DFT method. The calculations reveal linear correlations between isotropic NMR chemical shifts and PA value of modeled solid acids when steric effect from catalyst's framework is neglected. This suggests that ^{1}H and ^{15}N chemical shifts can be used as measures to probe intrinsic Brønsted acid strength where a larger ^{1}H or a smaller ^{15}N chemical shift corresponds to stronger acid strength. When taking into account steric effects, a linear correlation between ^{1}H chemical shift and O–H bond length can also be obtained regardless of the nature of the steric effect. ^{15}N chemical shift also exhibits linear correlation with O–H bond length except that the orientation of the C≡N bond is sharply deviated from its optimal orientation which results in ^{15}N chemical shift in a much larger magnitude. It is thus concluded that in combination with ^{1}H chemical shift, ^{15}N chemical shift may provide additional information on the nature of the steric effects and thus the structure of zeolite framework when acetonitrile is used as probe molecule.

Acknowledgements

Financial supports from China Postdoctoral Science Foundation (No. 20090451247) and National Natural Science Foundation of China (No. 20703058) are gratefully acknowledged. The authors thank Dr. Anmin Zheng and Mr. Zhen Wu for their technical support and helpful discussion. HLZ thanks National Sun Yat-sen University for a visiting research fellowship and their support in computing facilities.

References

[1] B.M. Reddy, M.K. Patil, Curr. Org. Chem. 12 (2008) 118.
[2] A. Bhan, E. Iglesia, Acc. Chem. Res. 41 (2008) 559.
[3] I.V. Kozhevnikov, J. Mol. Catal. A 305 (2009) 104.
[4] A. Corma, Chem. Rev. 95 (1995) 559.
[5] A. Gervasini, S. Bennici, A. Auroux, C. Guimon, Appl. Catal. A 331 (2007) 129.
[6] W.H. Chen, H.H. Ko, A. Sakthivel, S.J. Huang, S.H. Liu, A.Y. Lo, T.C. Tsai, S.B. Liu, Catal. Today 116 (2006) 111.
[7] K. Shimizu, T.N. Venkatraman, W.G. Song, Appl. Catal. A 225 (2002) 33.
[8] L.M. Peng, X.F. Guo, W.P. Ding, Chin. J. Magn. Reson. 26 (2009) 173.
[9] J.F. Haw, J.B. Nicholas, T. Xu, L.W. Beck, D.B. Ferguson, Acc. Chem. Res. 29 (1996) 259.
[10] J.H. Lunsford, W.P. Rothwell, W.X. Shen, J. Am. Chem. Soc. 107 (1985) 1540.
[11] H.L. Zhang, H.G. Yu, A.M. Zheng, S.H. Li, W.L. Shen, F. Deng, Environ. Sci. Technol. 42 (2008) 5316.
[12] J. Jänchen, J.H.M.C. Wolput, L.J.M. Ven, J.W. Haan, R.A. Santen, Catal. Lett. 39 (1996) 147.
[13] J. Huang, Y.J. Jiang, V.R.R. Marthala, Y.S. Ooi, J. Weitkarnp, M. Hunger, Micropor. Mesopor. Mater. 104 (2007) 129.
[14] A. Simperler, R.G. Bell, M.W. Anderson, J. Phys. Chem. B 108 (2004) 7142.
[15] A.M. Zheng, H.L. Zhang, L. Chen, Y. Yue, C.H. Ye, F. Deng, J. Phys. Chem. B 111 (2007) 3085.
[16] A.M. Zheng, S.J. Huang, W.H. Chen, P.H. Wu, H.L. Zhang, H.K. Lee, L.C. de Menorval, F. Deng, S.B. Liu, J. Phys. Chem. A 112 (2008) 7349.
[17] S. Hayashi, Chem. Lett. 38 (2009) 960.
[18] F. Marquez, H. Garcia, E. Palomares, L. Fernandez, A. Corma, J. Am. Chem. Soc. 122 (2000) 6520.
[19] J.C. Scaiano, H. Garcia, Acc. Chem. Res. 32 (1999) 783.
[20] M. Sierka, U. Eichler, J. Datka, J. Sauer, J. Phys. Chem. B 102 (1998) 6397.
[21] A.M. Zheng, H.L. Zhang, X. Lu, S.B. Liu, F. Deng, J. Phys. Chem. B 112 (2008) 4496.
[22] G.J. Kramer, R.A. Vansanten, C.A. Emeis, A.K. Nowak, Nature 363 (1993) 529.
[23] B. Delley, J. Phys. Chem. 92 (1990) 508.
[24] B. Delley, J. Phys. Chem. 94 (1991) 7245.
[25] B. Delley, J. Phys. Chem. 113 (2000) 7756.
[26] J.P. Perdew, Y. Wang, Phys. Rev. B 33 (1986) 8822.
[27] J.P. Perdew, Y. Wang, Phys. Rev. B 45 (1992) 13244.
[28] A.D. Becke, J. Chem. Phys. 98 (1993) 5648.
[29] R. Krishnan, J.S. Binkley, R. Seeger, J.A. Pople, J. Chem. Phys. 72 (1980) 650.
[30] K. Wolinski, J.F. Hinton, P. Pulay, J. Am. Chem. Soc. 112 (1990) 8251.
[31] M.J. Frisch, G.W. Trucks, H.B. Schlegel, G.E. Scuseria, M.A. Robb, J.R. Cheeseman, J.A. Montgomery Jr., T. Vreven, K.N. Kudin, J.C. Burant, J.M. Millam, S.S. Iyengar,

J. Tomasi, V. Barone, B. Mennucci, M. Cossi, G. Scalmani, N. Rega, G.A. Petersson, H. Nakatsuji, M. Hada, M. Ehara, K. Toyota, R. Fukuda, J. Hasegawa, M. Ishida, T. Nakajima, Y. Honda, O. Kitao, H. Nakai, M. Klene, X. Li, J.E. Knox, H.P. Hratchian, J.B. Cross, C. Adamo, J. Jaramillo, R. Gomperts, R.E. Stratmann, O. Yazyev, G.A. Voth, P. Salvador, J.J. Dannenberg, V.G. Zakrzewski, S. Dapprich, A.D. Daniels, M.C. Strain, O. Farkas, D.K. Malick, A.D. Rabuck, K. Raghavachari, J.B. Foresman, J.V. Ortiz, Q. Cui, A.G. Baboul, S. Clifford, J. Cioslowski, B.B. Stefanov, G. Liu, A. Liashenko, P. Piskorz, I. Komaromi, R.L. Martin, D.J. Fox, T. Keith, M.A. Al-Laham, C.Y. Peng, A. Nanayakkara, M. Challacombe, P.M.W. Gill, B. Johnson, W. Chen, M.W. Wong, C. Gonzalez, J.A. Pople, Gaussian 03, Revision B.05, Gaussian, Inc., Pittsburgh, PA, 2003.

[32] E.P. Hunter, S.G. Lias, J. Phys. Chem. Ref. Data 27 (1998) 413.

[33] J. Huang, Y.J. Jiang, V.R.R. Marthala, W. Wang, B. Sulikowski, M. Hunger, Micropor. Mesopor. Mater. 99 (2007) 86.

[34] J. Huang, Y.J. Jiang, V.R.R. Marthala, B. Thomas, E. Romanova, M. Hunger, J. Phys. Chem. C 112 (2008) 3811.

[35] H.B. Gao, Z.F. Zhang, NMR Principles and Experimental Methods, Wuhan University Press, Wuhan, 2008.